

**SYNTHESIS, X-RAY STRUCTURE
CHARACTERIZATION AND ANTIOXIDANT
ACTIVITIES OF SOME CHALCONE
DERIVATIVES CONTAINING 2-
CHLOROTHIOPHENE MOIETY**

NG WENG ZHUN

UNIVERSITI SAINS MALAYSIA

2021

**SYNTHESIS, X-RAY STRUCTURE
CHARACTERIZATION AND ANTIOXIDANT
ACTIVITIES OF SOME CHALCONE
DERIVATIVES CONTAINING 2-
CHLOROTHIOPHENE MOIETY**

by

NG WENG ZHUN

**Thesis submitted in fulfilment of the requirement
for the degree of
Master of Science**

March 2021

ACKNOWLEDGEMENT

I am really grateful that I am able to complete my master thesis on time. This thesis can be done because there are a lot of people who taught me with full of patient during my master project. First of all, I would take this opportunity to express my deepest gratitude to my supervisor, Assoc. Prof. Dr. Quah Ching Kheng for his professional guidance, very supportive to my research work and encouragement throughout the research journey. Besides, I am indebted to my co-supervisor, Dr. Suhana Arshad for her valuable suggestions and assisted me in this study. Not to forget to my field supervisor, Dr Mah Siau Hui who assisted me and taught me in analysis step of biological studies in my research.

I would like to take this opportunity to thank the Malaysia government for awarding me MyBrain15 (MyMASTER) scholarship. In addition, I would like to thanks to my laboratory mates for the invaluable helps and advice along the way. Last but not least, I would like to express my grateful to all my family members for their support and encouragement for all the time.

TABLE OF CONTENTS

ACKNOWLEDGEMENT.....	ii
TABLE OF CONTENTS.....	iii
LIST OF TABLES.....	vii
LIST OF FIGURES.....	ix
LIST OF ABBREVIATIONS.....	xvi
ABSTRAK.....	xviii
ABSTRACT.....	xx
CHAPTER 1 INTRODUCTION.....	1
1.1 X-ray Crystallography.....	1
1.2 Background and Problem Statement of the Research.....	4
1.3 Research Objectives.....	5
CHAPTER 2 Literature Review.....	6
2.1 Thiophene and Chlorothiophene.....	6
2.2 Chalcone.....	8
2.3 Spectroscopic Studies.....	12
CHAPTER 3 METHODOLOGY.....	16
3.1 Introduction.....	16
3.2 Sample Preparation.....	17
3.2.1 Chemicals.....	18
3.2.2 General Procedure for the Synthesis of 5-Chlorothiophen-2-yl Chalcone (Compounds 1a-1l).....	19
3.3 Spectroscopic Studies.....	20
3.4 Single Crystal X-ray Data Analysis.....	28
3.4.1 Crystal Selection.....	29
3.4.2 Crystal Mounting and Alignme.....	30
3.4.3 Data Collection.....	31

3.4.4	Data Reduction	33
3.4.5	Structure Determination.....	34
3.5	X-ray Diffractometer.....	35
3.5.1	Hardware.....	35
3.5.2	Software.....	37
3.5.3	SHELXTL Software Package.....	38
3.6	Hirshfeld Surface Studied.....	40
3.7	Antioxidant Evaluation.....	41
3.7.1	DPPH Radical Scavenging Assay.....	42
3.7.2	Nitric Oxide Scavenging Assay.....	43
3.7.3	Ferrous Ion Chelating Assay.....	44
3.7.4	Hydrogen Peroxide Radical Scavenging Assay.....	44
CHAPTER 4 RESULT AND DISCUSSION.....		46
4.1	Fourier Transform Infrared Spectroscopy (FT-IR) for Compound 1a-11	50
4.2	Nuclear Magnetic Resonance NMR (¹ H and ¹³ C).....	52
4.2.1	Proton NMR (¹ H).....	52
4.2.2	Carbon NMR (¹³ C).....	54
4.3	X-ray Structures of Chalcone Compounds 1a-11	55
4.3.1	(<i>E</i>)-1-(5-Chlorothiophen-2-yl)-3-(pyridin-2-yl)prop-2-en-1-one (1a).....	59
4.3.1(a)	Description of Compound 1a	59
4.3.1(b)	Hirshfeld Surfaces Analysis with Fingerprint Plots.....	63
4.3.2	(<i>E</i>)-1-(5-Chlorothiophen-2-yl)-3-(thiophen-2-yl)prop-2-en-1-one (1b).....	65
4.3.2(a)	Description of Compound 1b	65
4.3.2(b)	Hirshfeld Surfaces Analysis with Fingerprint Plots.....	70

4.3.3	(<i>E</i>)-1-(5-Chlorothiophen-2-yl)-3-(5-methylthiophen-2-yl)prop-2-en-1-one (1c).....	72
4.3.3(a)	Description of Compound 1c	72
4.3.3(b)	Hirshfeld Surfaces Analysis with Fingerprint Plots.....	75
4.3.4	(<i>E</i>)-1-(5-Chlorothiophen-2-yl)-3-(4-(methylthio)phenyl)prop-2-en-1-one (1d).....	77
4.3.4(a)	Description of Compound 1d	77
4.3.4(b)	Hirshfeld Surfaces Analysis with Fingerprint Plots.....	80
4.3.5	(<i>E</i>)-1-(5-Chlorothiophen-2-yl)-3-mesitylprop-2-en-1-one (1e).....	81
4.3.5(a)	Description of Compound 1e	81
4.3.5(b)	Hirshfeld Surfaces Analysis with Fingerprint Plots.....	85
4.3.6	(<i>E</i>)-3-(5-Bromothiophen-2-yl)-1-(5-chlorothiophen-2-yl)prop-2-en-1-one (1f).....	87
4.3.6(a)	Description of Compound 1f	87
4.3.6(b)	Hirshfeld Surfaces Analysis with Fingerprint Plots.....	91
4.3.7	(<i>E</i>)-3-(5'-Bromo-[2,2'-bithiophen]-5-yl)-1-(5-chlorothiophen-2-yl)prop-2-en-1-one (1g).....	93
4.3.7(a)	Description of Compound 1g	93
4.3.7(b)	Hirshfeld Surfaces Analysis with Fingerprint Plots.....	98
4.3.8	(<i>E</i>)-1-(5-Chlorothiophen-2-yl)-3-(4-(trifluoromethyl)phenyl)prop-2-en-1-one (1h).....	102
4.3.8(a)	Description of Compound 1h	102
4.3.8(b)	Hirshfeld Surfaces Analysis with Fingerprint Plots.....	106
4.3.9	(<i>E</i>)-1-(5-Chlorothiophen-2-yl)-3-(4-(trifluoromethoxy)phenyl)prop-2-en-1-one (1i).....	108
4.3.9(a)	Description of Compound 1i	108

4.3.9(b)	Hirshfeld Surfaces Analysis with Fingerprint Plots.....	111
4.3.10	(<i>E</i>)-1-(5-Chlorothiophen-2-yl)-3-(4-(dimethylamino)phenyl)prop-2-en-1-one (1j).....	112
4.3.10(a)	Description of Compound 1j	112
4.3.10(b)	Hirshfeld Surfaces Analysis with Fingerprint Plots.....	116
4.3.11	(<i>E</i>)-1-(5-Chlorothiophen-2-yl)-3-(4-(piperidin-1-yl)phenyl)prop-2-en-1-one (1k).....	118
4.3.11(a)	Description of Compound 1k	118
4.3.11(b)	Hirshfeld Surfaces Analysis with Fingerprint Plots.....	122
4.3.12	(<i>E</i>)-1-(5-Chlorothiophen-2-yl)-3-(2,3-dihydrobenzofuran-5-yl)prop-2-en-1-one (1l).....	124
4.3.12i	Description of Compound 1l	124
4.3.12ii	Hirshfeld Surfaces Analysis with Fingerprint Plots.....	128
4.4	Antioxidant Assays for Chalcone Compounds 1a-1l	130
CHAPTER 5 CONCLUSION AND FURTHER STUDIES.....		134
5.1	Thiophene Chalcone Moiety.....	134
5.2	Future Studies.....	136
REFERENCES.....		137

APPENDICES

LIST OF PUBLICATIONS

LIST OF TABLES

		Page
Table 2.1	The FT-IR bond values for heterocyclic chalcones containing halogen thiophene.....	14
Table 3.1	List of chemicals used for this research project.....	18
Table 4.1	The schematic diagram for synthesized compounds.....	46
Table 4.2	The FT-IR bond values for compound 1a - 1l	51
Table 4.3	Crystal data and structure refinement for compounds 1a – 1l ...	56
Table 4.4	Selected bond length and three torsion angles for compound 1a	60
Table 4.5	Hydrogen-bond geometry (Å, °) for (<i>E</i>)-1-(5-chlorothiophen-2-yl)-3-(pyridin-2-yl)prop-2-en-1-one (1a).....	61
Table 4.6	Selected bond length and three torsion angles for compound 1b	67
Table 4.7	Hydrogen-bond geometry (Å, °) for (<i>E</i>)-1-(5-chlorothiophen-2-yl)-3-(thiophen-2-yl)prop-2-en-1-one (1b).....	68
Table 4.8	Selected bond length and three torsion angles for compound 1c	73
Table 4.9	Hydrogen-bond geometry (Å, °) for (<i>E</i>)-1-(5-chlorothiophen-2-yl)-3-(5-methylthiophen-2-yl)prop-2-en-1-one (1c).....	73
Table 4.10	Selected bond length and three torsion angles for compound 1d	78
Table 4.11	Hydrogen-bond geometry (Å, °) for (<i>E</i>)-1-(5-chlorothiophen-2-yl)-3-(4-(methylthio)phenyl)prop-2-en-1-one (1d).....	79
Table 4.12	Selected bond length and three torsion angles for compound 1e	83
Table 4.13	Hydrogen-bond geometry (Å, °) for (<i>E</i>)-1-(5-chlorothiophen-2-yl)-3-mesitylprop-2-en-1-one (1e).....	83
Table 4.14	Selected bond length and three torsion angles for compound 1f	88

Table 4.15	Hydrogen-bond geometry (Å, °) for (<i>E</i>)-3-(5-bromothiophen-2-yl)-1-(5-chlorothiophen-2-yl)prop-2-en-1-one (1f).....	89
Table 4.16	Maximum deviation of rings in compound 1g	95
Table 4.17	Selected bond length and three torsion angles for compound 1g	95
Table 4.18	Hydrogen-bond geometry (Å, °) for (<i>E</i>)-3-(5'-bromo-[2,2'-bithiophen]-5-yl)-1-(5-chlorothiophen-2-yl)prop-2-en-1-one (1g).....	96
Table 4.19	Selected bond length and three torsion angles for compound 1h	103
Table 4.20	Hydrogen-bond geometry (Å, °) for (<i>E</i>)-1-(5-chlorothiophen-2-yl)-3-(4-(trifluoromethyl)phenyl)prop-2-en-1-one (1h).....	104
Table 4.21	Selected bond length and three torsion angles for compound 1i	109
Table 4.22	Hydrogen-bond geometry (Å, °) for (<i>E</i>)-1-(5-chlorothiophen-2-yl)-3-(4-(trifluoromethoxy)phenyl)prop-2-en-1-one (1i).....	110
Table 4.23	Selected bond length and three torsion angles for compound 1j	113
Table 4.24	Hydrogen-bond geometry (Å, °) for (<i>E</i>)-1-(5-chlorothiophen-2-yl)-3-(4-(dimethylamino)phenyl)prop-2-en-1-one (1j).....	114
Table 4.25	Selected bond length and three torsion angles for compound 1k	120
Table 4.26	Hydrogen-bond geometry (Å, °) for (<i>E</i>)-1-(5-chlorothiophen-2-yl)-3-(4-(piperidin-1-yl)phenyl)prop-2-en-1-one (1k).....	120
Table 4.27	Selected bond length and three torsion angles for compound 1l	125
Table 4.28	Hydrogen-bond geometry (Å, °) for (<i>E</i>)-1-(5-chlorothiophen-2-yl)-3-(2,3-dihydrobenzofuran-5-yl)prop-2-en-1-one (1l)....	126
Table 4.29	Inhibition results of chalcone compounds on different assays, including the reference drugs.....	131
Table 4.30	The IC ₅₀ values of compounds 1a , 1d and standard drug (EDTA) in FIC assay.....	132
Table 4.31	The IC ₅₀ values of compounds 1g , 1j , 1l and standard drugs (Ascorbic acid) in H ₂ O ₂ assay.....	133

LIST OF FIGURES

		Page
Figure 2.1	The chemical structures of (a) thiophene and (b) chlorothiophene.....	6
Figure 2.2	The chemical structure of chalcone.....	8
Figure 2.3	Compounds structure of 119b, 119c and 119j.....	9
Figure 2.4	The reaction scheme a series of 5-chlorothiophene chalcones.	10
Figure 2.5	Molecular structures of compounds 4a , 4b , 4c , 4d , 4e and 4f with atom numbering schemes.....	11
Figure 2.6	The compound (9) structure with atomic labelling scheme.....	12
Figure 3.1	Flow chart of research activities.....	17
Figure 3.2	Schematic diagram for synthesis of heterocyclic chalcone derivatives.....	19
Figure 3.3	Flow chart of X-ray crystallography technique.....	29
Figure 3.4	Crystals formed in a beaker (microscope view).....	30
Figure 3.5	Finest crystal (orange colour) was glued on the fibre optic tip of a copper pin.....	30
Figure 3.6	Goniometer head attached to the diffractometer.....	31
Figure 3.7	Diffraction patterns of (a) an amorphous sample and (b) a crystalline sample.....	32
Figure 3.8	The deviation histograms showing single crystal pattern.....	33
Figure 3.9	Bruker APEX II diffractometer.....	35
Figure 3.10	Goniometer modules (<i>APEX2 User Manual Version 1.27, 2005</i>).....	36
Figure 3.11	The APEX2 software diagram (<i>APEX2 User Manual Version 1.27, 2005</i>).....	38
Figure 3.12	Flow chat of SHELXTL programs.....	40
Figure 3.13	(a) Biotek Epoch 2 Microplate reader. (b) Genesys 10UV Scanning Spectrophotometer.....	42

Figure 4.1	FT-IR spectrum for compound 1d	52
Figure 4.2	Proton NMR spectrum for compound 1d	53
Figure 4.3	Carbon NMR spectrum for compound 1d	54
Figure 4.4	(a) <i>ORTEP</i> diagram with atomic labelling scheme of compound 1a with displacement ellipsoids are drawn at the 50% probability level, (b) three degrees of freedom τ in compound 1a	60
Figure 4.5	(a) A packing diagram of compound 1a showing the hydrogen bonds that link the symmetry related molecules into supramolecular layers parallel to <i>ac</i> -plane. (b) compound 1a is stabilized by weak intermolecular $\pi \cdots \pi$ interactions.....	62
Figure 4.6	The Hirshfeld surfaces mapped with normalized contact distance d_{norm} and fingerprint plots for specific pairs of atom types in compound 1a	64
Figure 4.7	The Hirshfeld surfaces mapped with normalized contact distance d_{norm} for visualizing the intermolecular interactions for compound 1a	64
Figure 4.8	(a) The Hirshfeld surfaces mapped with shape index and (b) curvedness of compound 1a	65
Figure 4.9	(a) <i>ORTEP</i> diagram with atomic labelling scheme of compound 1b with displacement ellipsoids are drawn at the 50% probability level, (b) four degrees of freedom τ were observed in compound 1b	67
Figure 4.10	(a) The crystal structure of compound 1b is stabilized by weak intermolecular C—H \cdots π interactions, involving the centroids of disordered thiophene rings, (b) the short contact of Cl—S2A.....	69
Figure 4.11	The Hirshfeld surfaces mapped with normalized contact distance d_{norm} and fingerprint plots for specific pairs of atom types in compound 1b	70
Figure 4.12	The Hirshfeld surfaces mapped with normalized contact distance d_{norm} for visualizing the intermolecular interactions for compound 1b	71
Figure 4.13	(a) The Hirshfeld surfaces mapped with shape index, (b) curvedness of compound 1b	71

Figure 4.14	(a) <i>ORTEP</i> diagram with atomic labelling scheme of compound 1c with displacement ellipsoids are drawn at the 50% probability level and (b) three degrees of freedom τ were observed in compound 1c	72
Figure 4.15	(a) The R_2^2 (14) inversion dimers form by weak intermolecular C—H···O hydrogen bonds, (b) weak intermolecular π ··· π interactions between chloro- and methyl-substituted thiophene rings.....	74
Figure 4.16	The Hirshfeld surfaces mapped with normalized contact distance d_{norm} and fingerprint plots for specific pairs of atom types in compound 1c	75
Figure 4.17	The Hirshfeld surfaces mapped with normalized contact distance d_{norm} for visualizing the intermolecular interactions for compound 1c	76
Figure 4.18	(a) The Hirshfeld surfaces mapped with shape index, (b) curvedness of compound 1c	76
Figure 4.19	(a) <i>ORTEP</i> diagram with atomic labelling scheme of compound 1d with displacement ellipsoids of 50% probability level, (b) three degrees of freedom τ in compound 1d	78
Figure 4.20	Hydrogen bond links the symmetry related molecules into extended chain parallel to <i>c</i> -axis.....	79
Figure 4.21	The Hirshfeld surfaces mapped with normalized contact distance d_{norm} and fingerprint plots for specific pairs of atom types in compound 1d	80
Figure 4.22	The Hirshfeld surfaces mapped with normalized contact distance d_{norm} for visualizing the intermolecular interactions for compound 1d	81
Figure 4.23	(a) <i>ORTEP</i> diagram with atomic labelling scheme of compound 1e with displacement ellipsoids are drawn at the 50% probability level, (b) three degrees of freedom τ in compound 1e	82
Figure 4.24	(a) The weak intermolecular C—H···O hydrogen bond of 1e , (b) the weak intermolecular C—H··· π interactions of 1e	84
Figure 4.25	The Hirshfeld surfaces mapped with normalized contact distance d_{norm} and fingerprint plots for specific pairs of atom types in compound 1e	85

Figure 4.26	The Hirshfeld surfaces mapped with normalized contact distance d_{norm} for visualizing the intermolecular interactions for compound 1e	86
Figure 4.27	(a) The Hirshfeld surfaces mapped with shape index, (b) curvedness of compound 1e	86
Figure 4.28	(a) <i>ORTEP</i> diagram with atomic labelling scheme of compound 1f with displacement ellipsoids are drawn at the 50% probability level, (b) three degrees of freedom τ were observed in compound 1f	88
Figure 4.29	(a) The hydrogen bonds link the symmetry related molecules into layers parallel $(10\bar{1})$, (b) weak intermolecular C—H \cdots Cl and C—H \cdots O hydrogen bonds into zigzag sheets parallel to $(10\bar{1})$. (c) weak intermolecular $\pi\cdots\pi$ interactions between chloro- and bromo-substituted thiophene rings.....	90
Figure 4.30	The Hirshfeld surfaces mapped with normalized contact distance d_{norm} and fingerprint plots for specific pairs of atom types in compound 1f	92
Figure 4.31	The Hirshfeld surfaces mapped with normalized contact distance d_{norm} for visualizing the intermolecular interactions for compound 1f	92
Figure 4.32	(a) The Hirshfeld surfaces mapped with shape index, (b) curvedness of compound 1f	93
Figure 4.33	(a) <i>ORTEP</i> diagram with atomic labelling scheme of compound 1g with displacement ellipsoids are drawn at the 50% probability level, (b) eight degrees of freedom τ were observed in compound 1g	94
Figure 4.34	(a) Molecules are connected by weak intermolecular C—H \cdots O hydrogen bonds into supramolecular chains along <i>a</i> -axis, (b) weak intermolecular $\pi\cdots\pi$ interactions between two thiophene rings.....	97
Figure 4.35	The Hirshfeld surfaces mapped with normalized contact distance d_{norm} and fingerprint plots for specific pairs of atom types in compound 1g (Molecule A).....	99
Figure 4.36	The Hirshfeld surfaces mapped with normalized contact distance d_{norm} for visualizing the intermolecular interactions for compound 1g (Molecule A).....	99
Figure 4.37	(a) The Hirshfeld surfaces mapped with shape index, (b) curvedness of compound 1g (Molecule A).....	100

Figure 4.38	The Hirshfeld surfaces mapped with normalized contact distance d_{norm} and fingerprint plots for specific pairs of atom types in compound 1g (Molecule <i>B</i>).....	100
Figure 4.39	The Hirshfeld surfaces mapped with normalized contact distance d_{norm} for visualizing the intermolecular interactions for compound 1g (Molecule <i>B</i>).....	101
Figure 4.40	(a) The Hirshfeld surfaces mapped with shape index, (b) curvedness of compound 1g (Molecule <i>B</i>).....	101
Figure 4.41	(a) <i>ORTEP</i> diagram with atomic labelling scheme of compound 1h with displacement ellipsoids are drawn at the 50% probability level, (b) three degrees of freedom τ were observed in compound 1h	103
Figure 4.42	(a) The molecules of compound 1h are connected by weak intermolecular C—H...F hydrogen bonds into $R_2^2(10)$ inversion dimers, (b) compound 1h is stabilized by weak intermolecular $\pi\cdots\pi$ interactions between thiophene and phenyl rings.....	105
Figure 4.43	The Hirshfeld surfaces mapped with normalized contact distance d_{norm} and fingerprint plots for specific pairs of atom types in compound 1h	106
Figure 4.44	The Hirshfeld surfaces mapped with normalized contact distance d_{norm} for visualizing the intermolecular interactions for compound 1h	107
Figure 4.45	(a) The Hirshfeld surfaces mapped with shape index, (b) curvedness of compound 1h	107
Figure 4.46	(a) <i>ORTEP</i> diagram with atomic labelling scheme of compound 1i with displacement ellipsoids are drawn at the 50% probability level, (b) three degrees of freedom τ were observed in compound 1i	109
Figure 4.47	Molecules are connected by weak intermolecular C—H...O hydrogen bonds and further connect by short contact of F...Cl into layers parallel to <i>ac</i> -plane.....	110
Figure 4.48	The Hirshfeld surfaces mapped with normalized contact distance d_{norm} and fingerprint plots for specific pairs of atom types in compound 1i	111
Figure 4.49	The Hirshfeld surfaces mapped with normalized contact distance d_{norm} for visualizing the intermolecular interactions for compound 1i	112

Figure 4.50	(a) <i>ORTEP</i> diagram with atomic labelling scheme of compound 1j with displacement ellipsoids are drawn at the 50% probability level, (b) three degrees of freedom τ in compound 1j	113
Figure 4.51	(a) Molecules are connected by weak intermolecular C—H···Cl and C—H···O hydrogen bonds into sheets parallel to (10 $\bar{1}$), (b) weak intermolecular π ··· π interactions between thiophene and phenyl rings in 1j	114
Figure 4.52	The Hirshfeld surfaces mapped with normalized contact distance d_{norm} and fingerprint plots for specific pairs of atom types in compound 1j	117
Figure 4.53	The Hirshfeld surfaces mapped with normalized contact distance d_{norm} for visualizing the intermolecular interactions for compound 1j	117
Figure 4.54	(a) The Hirshfeld surfaces mapped with shape index, (b) curvedness of compound 1j	118
Figure 4.55	(a) <i>ORTEP</i> diagram with atomic labelling scheme of compound 1k with displacement ellipsoids are drawn at the 50% probability level, (b) four degrees of freedom τ were observed in compound 1k	119
Figure 4.56	(a) Molecules are connected by weak intermolecular C—H···O hydrogen bonds into supramolecular layers parallel to <i>bc</i> -plane, (b) weak intermolecular C—H··· π interactions in compound 1k	121
Figure 4.57	The Hirshfeld surfaces mapped with normalized contact distance d_{norm} and fingerprint plots for specific pairs of atom types in compound 1k	122
Figure 4.58	The Hirshfeld surfaces mapped with normalized contact distance d_{norm} for visualizing the intermolecular interactions for compound 1k	123
Figure 4.59	(a) The Hirshfeld surfaces mapped with shape index, (b) curvedness of compound 1k	123
Figure 4.60	(a) <i>ORTEP</i> diagram with atomic labelling scheme of compound 1l with displacement ellipsoids are drawn at the 50% probability level, (b) three degrees of freedom τ were observed in compound 1l	125

Figure 4.61	(a) Molecules are connected by weak intermolecular C—H···O hydrogen bonds into layers parallel to $(10\bar{2})$, (b) weak intermolecular C—H··· π interactions in compound 1l , (c) weak intermolecular π ··· π interactions in compound 1l	127
Figure 4.62	The Hirshfeld surfaces mapped with normalized contact distance d_{norm} and fingerprint plots for specific pairs of atom types in compound 1l	129
Figure 4.63	The Hirshfeld surfaces mapped with normalized contact distance d_{norm} for visualizing the intermolecular interactions for compound 1l	129
Figure 4.64	(a) The Hirshfeld surfaces mapped with shape index, (b) curvedness of compound 1l	130
Figure 4.65	Comparison of IC ₅₀ values between compounds 1a , 1d and standard drugs (EDTA) in FIC assay.....	132
Figure 4.66	Comparison of IC ₅₀ values between compounds 1g , 1j , 1l and standard drugs (Ascorbic acid) in H ₂ O ₂ assay.....	133

LIST OF ABBREVIATIONS

3-D	Three-Dimensional
$\text{CuSO}_4 \cdot 5\text{H}_2\text{O}$	Copper Sulfate Pentahydrate
$\text{C}_4\text{H}_4\text{S}$	Thiophene
DNA	Deoxyribonucleic Acid
FT-IR	Fourier Transform Infrared
NMR	Nuclear Magnetic Resonance
DPPH	Diphenyl-2-picrylhydrazyl
NO	Nitric Oxide
FIC	Ferrous Ion Chelating
H_2O_2	Hydrogen Peroxide
CCD	Charge-Coupled Device
<i>R</i>	Residual-factor
<i>Goof/S</i>	Goodness of Fit
TMS	Tetramethylsilane
<i>I</i>	Characteristic Spin
δ	Chemical Shift
Ppm	Parts per Million
^1H	Proton
^{13}C	Carbon-13
<i>J</i>	Coupling Constant
PBS	Phosphate Buffer Saline
Fe^{2+}	Ferrous ions

OH•	Hydroxyl Radical
UV	Ultraviolet
CDCl ₃	Deuterated chloroform
ATR	Attenuated Total Reflection
MHz	Mega Hertz
SMART	Siemens Molecular Analysis Research Tools
$\bar{\nu}$	Wavenumber
GUI	Graphical User Interface
BIS	Bruker Instrument Service
SAINT	SAX Area-detector Integration (SAX-Siemens Analytical X-ray)
SADABS	Siemens Area Detector Absorption Correction
2-D	Two-Dimensional
vdW	Van der Waals
$\mu\text{g/mL}$	Microgram per Milliliter
mg/mL	Milligram per Millilitre
EDTA	Ethylenediaminetetraacetic Acid
FeCl ₂	Ferrous Chloride
wR	Weighted Reliability Index
ORTEP	Oak Ridge Thermal Ellipsoid Plot
IC ₅₀	Half Maximal Inhibitory Concentration
DFT	Density Functional Theory
NLO	Nonlinear Optics

**SINTESIS, PENCIRIAN STRUKTUR SINAR-X DAN KAJIAN
ANTIOKSIDAN TERHADAP BEBERAPA TERBITAN KALKON
MENGANDUNGI 2-KLOROTHIOPHENE**

ABSTRAK

Dalam projek ini, satu siri yang terdiri daripada dua belas sebatian heterosilik kalkon (**1a-1l**) yang mengandungi 2-klorothiophene telah disintesis dan dihaburkan melalui penyejatan secara perlahan. Semua struktur hablur telah dicirikan dengan analisis spektroskopi FTIR, NMR, dan seterusnya ditentukan dengan teknik kristalografi sinar-X hablur tunggal. Selain itu, penilaian kegiatan aktiviti antioksidan bagi semua sebatian telah dijalankan dengan empat ujian termasuk 2, 2-difenil-1-picrylhydrazyl (DPPH), ferrous ion chelating (FIC), nitrik oksida (NO) and hidrogen peroxide (H₂O₂). Sembilan sebatian telah dicirikan dalam kumpulan ruang monoklinik $P2_1/c$ ($P2_1/n$), Cc dan Pc . Dua sebatian telah dicirikan dalam kumpulan ruang triklinik $P\bar{1}$ dan satu dalam ortorombik $Pbca$. Semua sebatian kalkon yang membina daripada dua fenil yang disambung dengan pengambung C=C-C(=O)-C dan membentuk konformasi trans dari ikatan berganda (C=C). Majoriti sebatian adalah penghubung hampir mendatar kecuali sebatian (*E*)-1-(5-klorothiophen-2-yl)-3-mesitilprop-2-en-1-one (**1e**) dan (*E*)-3-(5'-bromo-[2,2'-bithiophen]-5-yl)-1-(5-klorothiophen-2-yl)prop-2-en-1-one (**1g**). Sebatian (*E*)-1-(5-klorothiophen-2-yl)-3-(thiophen-2-yl)prop-2-en-1-one (**1b**) dan (*E*)-1-(5-klorothiophen-2-yl)-3-(4-(trifluorometil)fenil)prop-2-en-1-one (**1h**) yang mengandungi struktur bercelaru. Semua sebatian mempamerkan kedua-dua ikatan hidrogen konvensional dan bukan konvensional kecuali sebatian (*E*)-1-(5-klorothiophen-2-yl)-3-(4-(metilthio)fenil)prop-2-en-1-one (**1d**) dan (*E*)-1-(5-klorothiophen-2-yl)-3-(4-(trifluorometoksi)fenil)prop-2-en-1-one (**1i**). Berdasarkan

keputusan penghambatan antioksidan, sebatian (*E*)-1-(5-klorothiophen-2-yl)-3-(piridin-2-yl)prop-2-en-1-one (**1a**) dan (*E*)-1-(5-klorothiophen-2-yl)-3-(4-(metilthio)fenil)prop-2-en-1-one (**1d**) aktif terhadap ujian FIC. Manakala, sebatian (*E*)-1-(5-klorothiophen-2-yl)-3-(4-(metilthio)fenil)prop-2-en-1-one (**1d**) menunjukkan kekuatan kelat yang lebih tinggi daripada asam etilenadiaminatetraasetat (ubat standard).

**SYNTHESIS, X-RAY STRUCTURE CHARACTERIZATION AND
ANTIOXIDANT ACTIVITIES OF SOME CHALCONE DERIVATIVES
CONTAINING 2-CHLOROTHIOPHENE MOIETY**

ABSTRACT

A total of twelve heterocyclic chalcone compounds (**1a-1l**) containing 2-chlorothiophene moieties were synthesized using Claisen Schmidt Condensation process and were crystallized by slow evaporation methods. The postulate structure of these heterocyclic chalcone compounds were elucidated by FT-IR and NMR spectral analyses, followed by single crystal X-ray diffraction technique. Besides, the antioxidant potential of all compounds was evaluated using four different types of antioxidant assay which include 2, 2-diphenyl-1-picrylhydrazyl (DPPH), ferrous ion chelating (FIC), nitric oxide (NO) and Hydrogen Peroxide (H₂O₂) radical scavenging assay. Nine compounds are crystallized in monoclinic space group with four compounds in *P2₁/c*, three compounds in *P2₁/n* and two compounds in *Cc* and *Pc*. Another, two compounds are crystallized in triclinic space group *P $\bar{1}$* and one in orthorhombic space group *Pbca*. All the chalcone molecules are constructed by two individual rings which are interconnected by a C=C-C(=O)-C enone bridge and form a *trans* configuration with respect to the C=C double bond. The majority of the compounds is adopted to a nearly-planar conformation except compound (*E*)-1-(5-chlorothiophen-2-yl)-3-mesitylprop-2-en-1-one (**1e**) and (*E*)-3-(5'-bromo-[2,2'-bithiophen]-5-yl)-1-(5-chlorothiophen-2-yl)prop-2-en-1-one (**1g**). Two molecular structures, (*E*)-1-(5-chlorothiophen-2-yl)-3-(thiophen-2-yl)prop-2-en-1-one (**1b**) and (*E*)-1-(5-chlorothiophen-2-yl)-3-(4-(trifluoromethyl)phenyl)prop-2-en-1-one (**1h**) are disordered structure. All compounds exhibit both conventional and non-conventional

hydrogen bonds except compounds (*E*)-1-(5-chlorothiophen-2-yl)-3-(4-(methylthio)phenyl)prop-2-en-1-one (**1d**) and (*E*)-1-(5-chlorothiophen-2-yl)-3-(4-(trifluoromethoxy)phenyl)prop-2-en-1-one (**1i**). Based on the antioxidant inhibition results, it shows that compounds (*E*)-1-(5-chlorothiophen-2-yl)-3-(pyridin-2-yl)prop-2-en-1-one (**1a**) and (*E*)-1-(5-chlorothiophen-2-yl)-3-(4-(methylthio)phenyl)prop-2-en-1-one (**1d**) are active toward FIC assay. Meanwhile, compound (*E*)-1-(5-chlorothiophen-2-yl)-3-(4-(methylthio)phenyl)prop-2-en-1-one (**1d**) shows higher chelating power than the standard drugs (EDTA) in IC₅₀ test.

INTRODUCTION

1.1 X-ray Crystallography

In general, crystals are formed from basis such as atoms, molecules and ions that fit into lattice, the three-dimensional repeating patterns. The word of “crystallography” in science refer to determination of the arrangement of atoms in a crystalline solid. With the invention of X-ray, the inner structure of crystalline material which includes types and positions of all atoms can be analysed through X-ray diffraction technique. The main purpose of using X-ray is due to its wavelength is comparable to the size of atoms and it possesses high energy that enable it to penetrate the matter. This X-ray crystallography technique helps the scientist to investigate the structures and therefore to understand and study the behaviour of the matters. Modification of structures is widely done in the fields of chemistry, pharmacology, molecular biology, materials science and mineralogy to enhance the properties of the structure.

X-ray crystallography has been using for more than a hundred year. In 1895, Wilhelm Roentgen, a German professor of physics, who is the first person to discover electromagnetic radiation in a short wavelength range which known as X-rays. He was then honoured with the first Nobel Prize in Physics in 1901 for his remarkable achievement in discovery of X-rays (Wilhelm Röntgen, 2010). In 1912, another German physicist, Max von Laue, continues to work on the development of X-ray crystallography. He postulated that atoms in a single crystal have a regular and periodic pattern with interatomic distances in the order of about 1 Å. He also made an assumption that structure of a single crystal can be discovered using diffraction patterns of X-rays, much like a gradient in an infrared spectrometer that can diffract

infrared light. This statement was then confirmed by two remarkable researchers, Walter Friedrich and Paul Knipping, who successfully photographed the diffraction pattern associated with the X-ray radiation of crystalline structure, $\text{CuSO}_4 \cdot 5\text{H}_2\text{O}$. A few years later in north England, the British physicist Sir William Henry Bragg and his son William Lawrence Bragg were jointly awarded Nobel Prize in Physics in year 1915 due to their prestige contribution in development of X-ray crystallography. They discovered that diffracted X-rays can be utilized to detect the arrangement of atoms inside a crystal through the famous simple mathematical equation, Bragg's law (*Bragg & William Lawrence, 2009*). This discovery gets the science of X-ray crystallography started. The X-ray crystallographic technique was then refined by the blooming of theories and mathematic equations such as, structure factor, Fourier synthesis, direct methods, Patterson method etc. In recent year, X-ray crystallographic technique is widely employed in characterizing the structure of new compounds.

Spectroscopy is a technique to study the interactions occur between the matter and the electromagnetic radiation. It enables researcher to characterize the studied compounds through combination of different spectroscopy tools. Therefore, the invention of spectroscopy tools has enhanced the development of organic chemistry and they are widely used in the determination of the structure of organic compounds. Two types of spectroscopy tools are used in this research project to characterize the molecular structure which include Fourier transform infrared (FT-IR) spectroscopy and the nuclear magnetic resonance (NMR) spectroscopy (proton and carbon-13).

Antioxidant is related to free radical in human body cell. Free radicals is an unstable atom that it shells is not fully filled up by electron and this atom may bond with another atom to complete the shell to reach stable state. One of the examples is

oxygen molecules in human body split into unpaired electrons (free radicals), and bond with other atoms or molecules. This continuous reaction process is oxidative stress, which can damage human body cells and tend to a range of diseases such as central nervous system diseases, cardiovascular diseases and cancer. To reduce the free radicals in human body, antioxidant is needed to prevent the oxidation of other molecules. To prevent this, antioxidant will donate an electron to free radicals and reducing their reactivity to others atoms or molecules (V. Lobo *et. al.*, 2010). To develop the new antioxidant agent, there are many standardized analytic methods such as 2, 2-diphenyl-1-picrylhydrazyl (DPPH) radical scavenging assay, nitric oxide (NO) scavenging assay, ferrous ion (FIC) chelating assay and hydrogen peroxide (H₂O₂) radical scavenging assay.

The chalcone derivatives containing 2-chlorothiophene moiety which consist of aromatic (thiophene) ketone and an enone that forms the central core for a variety of important biological compounds, which are known collectively as chalcones or chalconoids. The thiophene is a heterocyclic compound that consists of a planar five members ring bearing the formula C₄H₄S with four carbon atoms and one sulphur atom. Thiophene can be obtained through the isolation of natural material such as coal tar and petroleum (National Centre for Biotechnology Information, 2019). Nowadays, thiophene can be prepared commercially from the chemical process by using butane and sulphur dioxide. On the other hand, chalcone can be prepared by an aldol condensation between benzaldehyde and acetophenone in the presence of sodium hydroxide as a catalyst.

1.2 Background and Problem Statement of the Research

Nowadays, several lifestyle, stress and environment factors will boost the number of free radicals in human body and cause oxidative stress which can potentially damage body DNA, trigger heart disease and other diseases (V. Lobo *et. al.*, 2010). To prevent free radical exceed antioxidants, the development of better antioxidant agents is still carried on by worldwide researchers (Kurutas, 2016). Heterocyclic chalcone is one of the well-known compounds which have attracted the attentions of scientists who work in the field of pharmaceuticals especially antioxidant assay (Wang *et. al.*, 2018). The antioxidant abilities of these heterocyclic chalcone compounds can be improved through the modification of structures and compounds to offer a higher degree of diversity (Yerragunta *et. al.*, 2013). A non-destructive method (X-ray crystallography method) is selected for determining the crystal structures of these modified heterocyclic chalcone compounds because it able to generates three-dimensional structure to provide physical properties of the crystal structure. The physical properties of the crystal packing is directly impact to the polymorphism of the drugs design.

In this research project, twelve new heterocyclic thiophene chalcone compounds are synthesized and crystallized in order to study the interactions between the molecules inside the crystal structures as well as the effect of different substituent groups towards the antioxidant abilities. Hirshfeld surface study serves as a visualisation tool to study the interactions and connections between molecules.

1.3 Research Objectives

There are 3 objectives in this research which include:

- i. To synthesize and characterize the chlorothiophene derivatives using spectroscopic techniques.
- ii. To analyze the three-dimensional crystal structures using X-ray crystallography method and Hirshfeld surfaces analysis with fingerprint plots.
- iii. To assess the antioxidant potential on these novel chlorothiophene chalcones.

Literature Review

2.1 Thiophene and Chlorothiophene

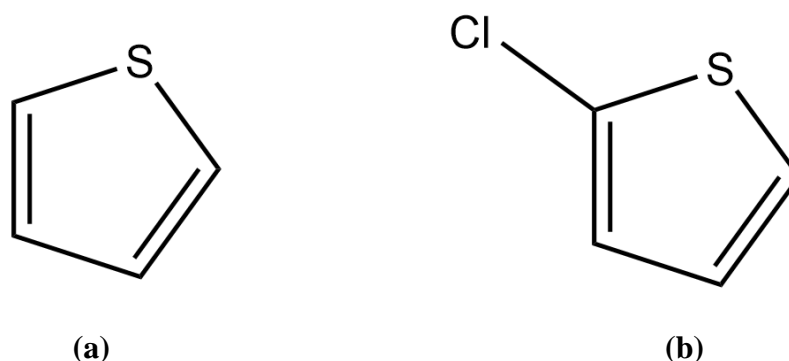


Figure 2.1 The chemical structures of (a) thiophene and (b) chlorothiophene.

Thiophene and its substituted derivatives are very important class of heterocyclic compound that consists of a planar five members ring bearing the formula C_4H_4S with four carbon atoms and one sulphur atom (Figure 2.1a) which showed interesting applications in the field of medicinal chemistry. It has made an indispensable anchor for medicinal chemists to produce combinatorial library and carry out exhaustive efforts in the search of lead molecules. It has been reported to possess a wide range of therapeutic properties with diverse applications in medicinal chemistry and material science, attracting great interests in industry as well as academia (Shah & Verma, 2018). Thiophene can be obtained through the isolation of natural material such as coal tar and petroleum (National Centre for Biotechnology Information, 2019). Nowadays, thiophene can be prepared commercially from the chemical process by using butane and sulphur dioxide. The sulphur element in the thiophene has been well recognized as an antifungal agent through many studies (Richard *et. al.*, 2004). Besides, thiophenes are widely used as building block in many agrochemicals and pharmaceuticals (Chu *et. al.*, 2018; Modzelewska *et. al.*, 2006; Debrashi Kar *et. al.*, 2017; Lahtchev *et. al.*, 2008 and Gopi *et. al.*, 2016). Besides, the

sulphur element in the thiophene containing heterocyclic scaffold, has emerged as one of the relatively well-explored scaffold for the development of library of molecules having potential anticancer profile. Thiophene analogs have been reported to bind with a wide range of cancer-specific protein targets, depending on the nature and position of substitutions (Archana *et. al.*, 2020). Furthermore, thiophene moiety has been recognized as a toxicophore because of the potential of oxidative bio-activation leading to electrophilic species. The introduction of bulky or electron-withdrawing groups at the α -carbon to the sulphur atom has the potential to reduce or eliminate bio-activation (Chen *et. al.*, 2011).

On the other hand, the synthesis of chlorothiophene (Figure 1.1b) from the substitution of chlorine atom into the thiophene ring enhances the pharmaceutical properties such as anti-inflammatory (Revannasiddaiah, *et. al.*, 2014), analgesic activity (Surendra & Muni, 2003) and antioxidant agent (Chidan *et. al.*, 2013). The pharmacological potential of chlorothiophene in the medicinal chemistry encourages the scientists to study on its derivatives. Besides, chlorothiophene-amides exhibit a strong anti-thrombotic effect which may use for the therapy and prophylaxis of cardiovascular disorders like thromboembolic diseases or restenosis (Steinhagen *et. al.*, 2009). Furthermore, the derivatives of chlorothiophene chalcone is one of the fascinating material which exhibits high nonlinear optical coefficient and good crystallizability (Ganapayya *et. al.*, 2012). Therefore, the synthesis and characterization of novel thiophene moieties with wider therapeutic activity is a topic of interest for the medicinal chemist to synthesize and investigate new structural prototypes with more effective pharmacological activity.

2.2 Chalcone

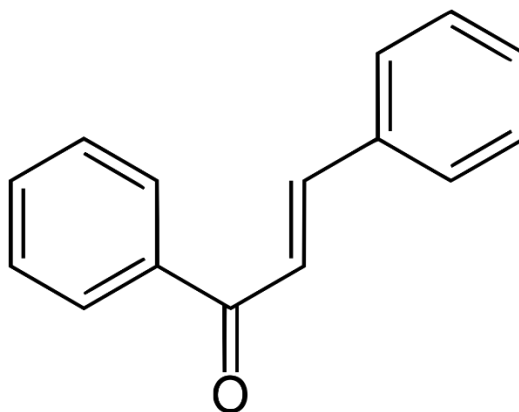


Figure 2.2 The chemical structure of chalcone

Chalcones are a group of plant-derived polyphenolic compounds belonging to the flavonoids family and which construct by aromatic ketones and enones that forms the central core for a variety of important biological compounds, which are known collectively as chalcones or chalconoids. Their physicochemical properties seem to define the extent of their biological activity. One of the physicochemical properties of chalcones is anticancer effects. Although parent chalcones consist of two aromatic rings joined by a three-carbon α,β -unsaturated carbonyl system, various synthetic compounds possessing heterocyclic rings like pyrazole and indole are well known and proved to be effective anticancer agents. (Valavanidis & Vlachogianni, 2013). Chalcone as one of the member of flavonoids, they are considered as open-chain flavonoids found abundantly in edible plants. Many heterocycles of biological importance, such as pyrazolines, flavones, 1,4-diketones and benzothiazepine can be synthesized using chalcones as key precursors. The two rings A and B which are linked by α, β -unsaturated carbonyl system are the unique features of chalcones as antidiabetic drugs (Raut *et. al.*, 2016).

Detsi *et. al.* (2020) had synthesized a series of 2-hydroxychalcones and evaluated their inhibitory activity against soybean lipoxygenase. Lipoxygenases are iron-containing enzymes widely distributed in plant and animals. They catalyse the oxidation of polyunsaturated fatty acids such as linoleic acid (plant) and arachidonic acid (mammals) at specific positions to hydroperoxides. Lipoxygenase inhibitors are of interest due to the implication of the enzyme to various pathophysiological conditions. The majority of lipoxygenase inhibitors are antioxidants or free radical scavengers, since lipoxygenation occurs via a carbon centered radical and therefore these compounds can inhibit radical formation or trap it once formed. The lipoxygenase inhibition revealed compounds 119b, 119c and 119j (Figure 2.3) as the most potent having IC_{50} of 52.5, 56 and 53 μM , respectively. This result is comparable with nordihydroguaiacetic acid (IC_{50} of 40 μM) and far better than caffeic acid (IC_{50} of 600 μM).

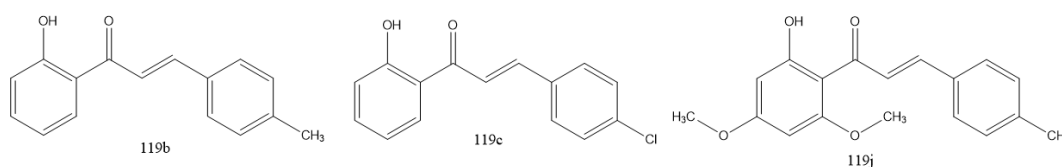


Figure 2.3 Compounds structure of 119b, 119c and 119j.

Kumar *et. al.*, (2013) have studied a series of 5-chlorothiophene chalcones and evaluate their in vitro antioxidant activity which includes DPPH Radical Scavenging Assay, ABTS Radical Scavenging Assay, Ferric Reducing Antioxidant Power (FRAP) Assay and Cupric Ion Reducing Antioxidant Capacity (CUPRAC) Assay. The new series of chalcones have been designed (Figure 2.4) and synthesized by the reaction of 2-acetyl-5-chlorothiophene with substituted benzaldehydes in presence of catalytic

amount of NaOH in methanol. The molecular structures of compounds **4a**, **4b**, **4c**, **4d**, **4e** and **4f** with atom numbering schemes is shown in Figure 2.5.

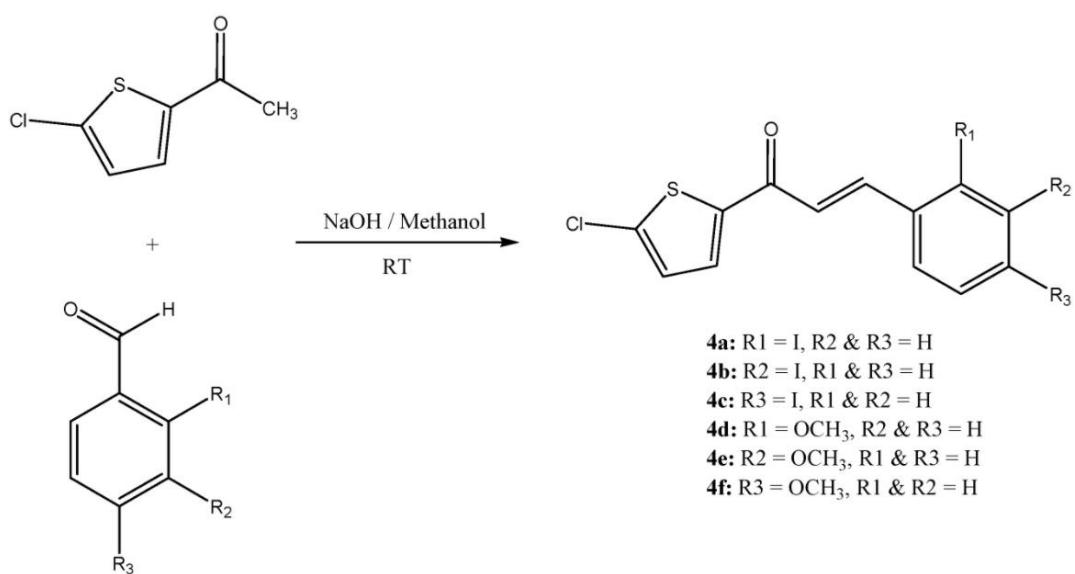


Figure 2.4 The reaction scheme a series of 5-chlorothiophene chalcones.

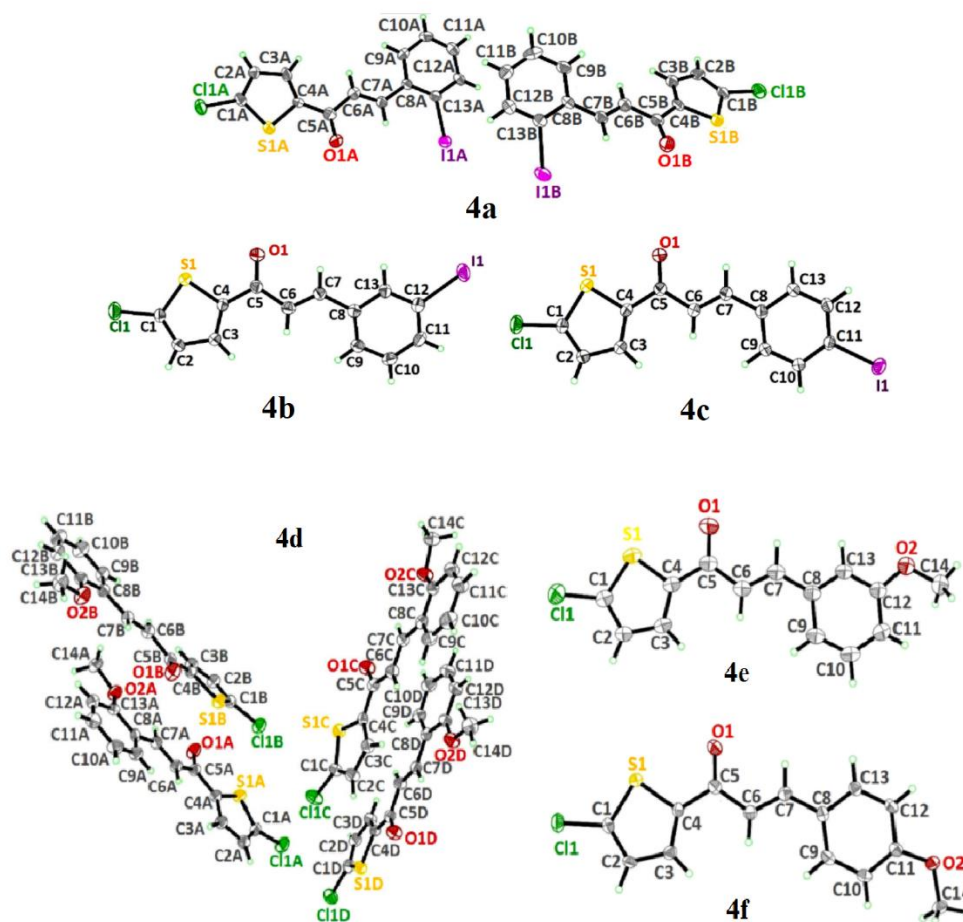


Figure 2.5 Molecular structures of compounds **4a**, **4b**, **4c**, **4d**, **4e** and **4f** with atom numbering schemes.

The report showed the compounds display mild to good antioxidant properties, which is due to the presence of electronegative $-I$ and electron donating $-OCH_3$ substituent at different positions on the phenyl ring. The increasing order of antioxidant activity of the synthesized compounds follows the order **4f** > **4d** > **4e** > **4b** > **4a** > **4c**. The present study revealed that (1) the influence of the nature of the functional linkage (electron withdrawing and electron donating groups) and (2) the position of the substituent on the phenyl ring of 5-chlorothiophene chalcones are crucial for the exhibited antioxidant activities.

2.3 Spectroscopic Studies

A series of heterocyclic chalcones containing halogen thiophene was discussed by Al-Maqtari *et. al.* (2015). The Fourier Transform Infrared (FT-IR) spectroscopy and the Nuclear Magnetic Resonance (NMR) spectroscopy (proton and carbon-13) data for these series of chalcone was shown in Table 2.1. Based on the results, sp^2 aromatic carbon (=C-H) are present in all compounds with the absorption bands higher than 3000 cm^{-1} ($3078 - 3102\text{ cm}^{-1}$). A very strong band of the carbonyl group (C=O) is shifted to lower frequencies ($1634\text{ cm}^{-1} - 1645\text{ cm}^{-1}$) which is due to the conjugation of C=C in the enone bridge. The C=C stretching bands for aromatic rings of the thiophene and benzene rings occur in pairs at the frequency's range of $1512 - 1562\text{ cm}^{-1}$ and $1524 - 1585\text{ cm}^{-1}$, respectively. Meanwhile, at the low region, a strong C-Cl stretching absorption band for all compounds are observed in the frequency ranges of $1013 - 1020\text{ cm}^{-1}$.

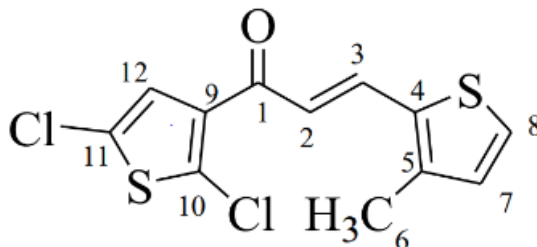


Figure 2.6 The compound (9) structure with atomic labelling scheme.

The ^1H NMR spectrum exhibited six signals integrating for eight protons (3 for the thiophene rings, 2 for α,β -unsaturated double bond and 3 for methyl protons). The vinylic proton, H-3 at δ 7.98 (1H, d, $J = 15.4\text{ Hz}$) was coupled with H-2 at δ 7.12 (1H, d, $J = 15.4\text{ Hz}$) suggested that they are in trans-orientation. The ^{13}C NMR and DEPT NMR spectra of chalcone (9) (Figure 2) showed the presence of twelve carbons, consisted of five quaternary (C-4, C-5, C-9, C-10, C-11) and deshielded carbon signal

at δ 183.0ppm was assigned to carbonyl group (C=O) at (C-1).The olefinic carbon C-2 and C-3 were observed at 121.4 and 136.2 ppm, respectively.

Table 2.1 The FT-IR bond values for heterocyclic chalcones containing halogen thiophene.

Type of bond Compound	Ar-H (cm ⁻¹)	C=O (cm ⁻¹)	Ar-C=C (cm ⁻¹)	C-Cl (cm ⁻¹)	¹ H NMR (CDCl ₃)	¹³ C NMR (CDCl ₃)
(<i>E</i>)-3-(5-Bromothiophen-2-yl)-1-(2,5-dichlorothiophen-3-yl)-2-propen-1-one (8)	3078	1644	1512, 1579	1020	δ 7.07 (1H, d, J = 4 Hz, H-5), δ 7.08 (1H, d, J = 15.2 Hz, H-2), δ 7.12 (1H, d, J = 4 Hz, H-6), δ 7.19 (1H, s, H-11), δ 7.76 (1H, d, J = 15.2 Hz, H-3)	δ 117.2 (C-7), δ 122.6 (C-5), δ 127.1 (C-11), δ 127.1 (C-8), δ 131.3 (C-9), δ 131.5 (C-2), δ 132.9 (C-6), δ 136.6 (C-3), δ 137.6 (C-10), δ 141.6 (C-4), δ 182.8 (C-1)
(<i>E</i>)-1-(2,5-Dichlorothiophen-3-yl)-3-(3-methylthiophen-2-yl)-2-propen-1-one (9)	3102	1640	1562, 1524	-	δ 2.39 (3H, s, H-6), δ 6.92 (1H, d, J = 4.8 Hz, H-7), δ 7.12 (1H, d, J = 15.4 Hz, H-2), δ 7.2 (1H, s, H-12), δ 7.35 (1H, d, J = 4.8 Hz, H-8), δ 7.9 (1H, d, J = 15.4 Hz, H-3)	δ 14.3 (C-6), δ 121.4 (C-2), δ 126.9 (C-9), δ 127.1 (C-12), δ 128.2 (C-8), δ 131.0 (C-7), δ 131.6 (C-5), δ 134.3 (C-10), δ 136.2 (C-3), δ 137.9 (C-11), δ 143.5 (C-4), δ 183.0 (C-1)
(<i>E</i>)-1-(5-Chlorothiophen-2-yl)-3-(3-methylthiophen-2-yl)-2-propen-1-one (10)	3079	1634	1523, 1572	1013	δ 2.42 (3H, s, H-6), δ 6.94 (1H, d, J = 4.8 Hz, H-11), δ 7.02 (1H, d, J = 4.0 Hz, H-8), δ 7.07 (1H, d, J = 15.2 Hz, H-2), δ 7.35 (1H, d, J = 5.2 Hz, H-7), δ 7.64 (1H, d, J = 4.0 Hz, H-10), δ 8.06 (1H, d, J = 15.2 Hz, H-3)	δ 14.3 (C-6), δ 118.2 (C-2), δ 127.6 (C-7, C-8), δ 130.8 (C-10), δ 131.5 (C-11), δ 134.2 (C-3), δ 135.3 (C-5), δ 139.4 (C-12), δ 143.3 (C-4), δ 144.4 (C-9), δ 180.7 (C-1)
(<i>E</i>)-3-(5-Bromothiophen-2-yl)-1-(5-chlorothiophen-2-yl)-2-propen-1-one (11)	3083	1645	1528, 1585	1014	δ 7.12 (1H, d, J = 4.8 Hz, H-6), δ 7.19 (1H, d, J = 15.2 Hz, H-2), δ 7.21 (1H, s, H-11), δ 7.39 (1H, d, J = 3.6 Hz, H-5), δ 7.47 (1H, d, J = 5.2 Hz, H-7), δ 7.90 (1H, d, J = 15.2 Hz, H-3)	-

Table 2.1 *Cont.*

Type of bond Compound	Ar-H (cm ⁻¹)	C=O (cm ⁻¹)	Ar-C=C (cm ⁻¹)	C-Cl (cm ⁻¹)	¹ H NMR (CDCl ₃)	¹³ C NMR (CDCl ₃)
(<i>E</i>)-1-(2,5-Dichlorothiophen-3-yl)-3-(thiophen-2-yl)-2-propen-1-one (12)	3091	1643	1525, 1567	1018	δ 7.12 (1H, d, J = 5.0 Hz, H-6), δ 7.19 (1H, d, J = 15.2 Hz, H-2), δ 7.21 (1H, s, H-11), δ 7.39 (1H, d, J = 3.6 Hz, H-5), δ 7.47 (1H, d, J = 5.0 Hz, H-7), δ 7.90 (1H, d, J = 15.2 Hz, H-3)	-
(<i>E</i>)-1-(5-Chlorothiophen-2-yl)-3-(thiophen-2-yl)-2-propen-1-one (13)	3080	1637	1528, 1574	1014	δ 7.03 (1H, d, J = 4 Hz, H-5), δ 7.13 (1H, t, J = 4 Hz, H-6), δ 7.134 (1H, d, J = 15.2 Hz, H-2), δ 7.40 (1H, d, J = 3.6 Hz, H-10), δ 7.47 (1H, d, J = 4.8 Hz, H-7), δ 7.65 (1H, d, J = 4.0 Hz, H-9), δ 7.98 (1H, d, J = 15.2 Hz, H-3).	-

Chapter 3

METHODOLOGY

3.1 Introduction

In this research, 12 chalcone compounds were synthesized through Claisen-Schmidt condensation reaction and were recrystallized into single crystals by slow evaporation process. The crystal structures for all the compounds were characterized using several methods such as X-ray crystallography, FT-IR, NMR spectroscopy and Hirshfeld surface analysis. Next, all compounds were evaluated by 4 types of antioxidant assays which include 2, 2-diphenyl-1-picrylhydrazyl (DPPH) radical scavenging assay, nitric oxide (NO) scavenging assay, ferrous ion (FIC) chelating assay and hydrogen peroxide (H₂O₂) radical scavenging assay.

The research process for this project is classified into five steps which are sample preparation, spectroscopy studies, single crystal analysis, Hirshfeld surface studies and antioxidant analysis (Figure 3.1). Each step of the research activities will be further deliberated in the following sections.

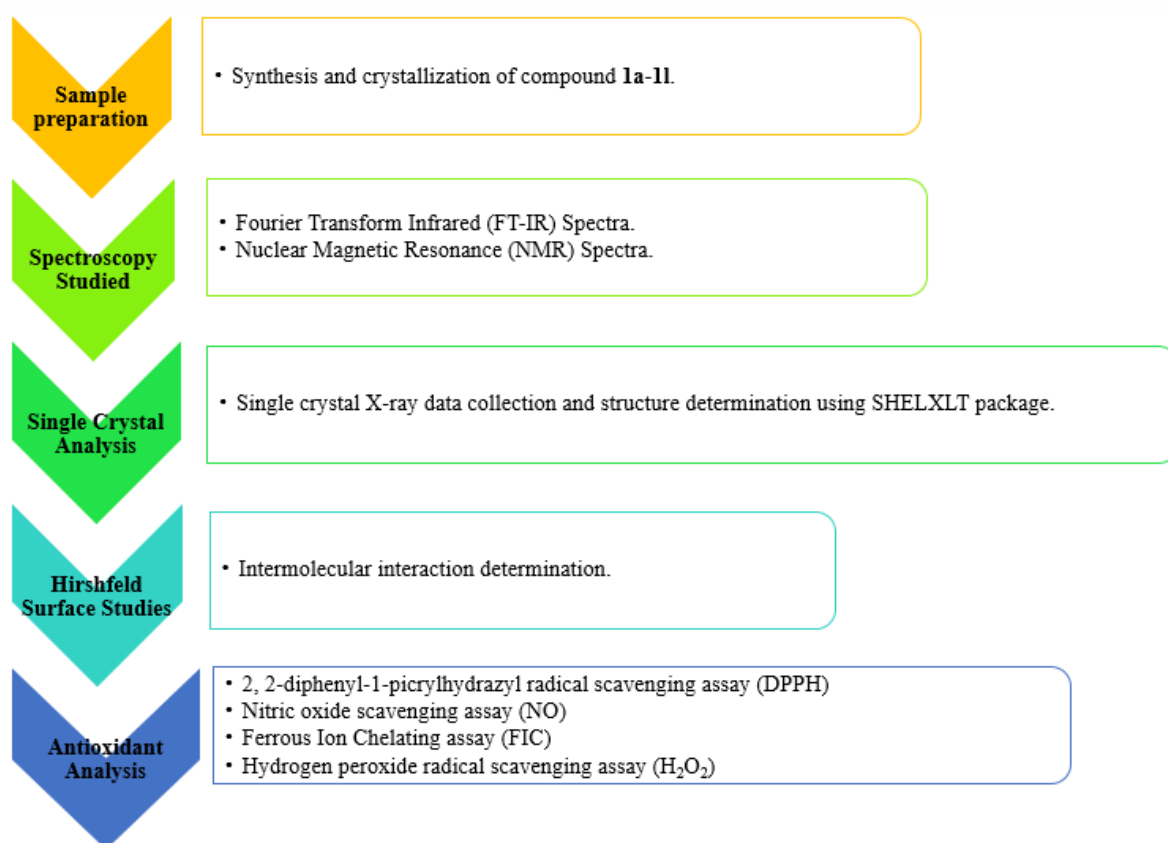


Figure 3.1 Flow chart of research activities.

3.2 Sample Preparation

In this research, twelve samples have been synthesized with good yield through Claisen Schmidt Condensation process at School of Physics (X-ray Crystallography Unit), Universiti Sains Malaysia. All of these samples were crystallized using slow evaporation methods.

3.2.1 Chemicals

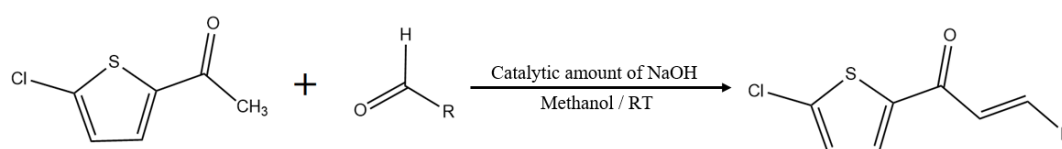
All chemicals consumed in this research project are used directly without any purification and are listed in Table 3.1.

Table 3.1 List of chemicals used for this research project.

Chemical name	Molecular Formula	Purity (%)	Manufacturer
2-Acetyl-5-chlorothiophene	C ₆ H ₅ ClOS	99 %	Sigma Aldrich
2-Pyridinecarbaldehyde	C ₆ H ₅ NO	99 %	Merck
Thiophene-2-carbaldehyde	C ₅ H ₄ OS	98 %	Merck
5-Methylthiophene-2-carbaldehyde	C ₆ H ₆ OS	98 %	Merck
4-Methylthiobenzaldehyde	C ₈ H ₈ OS	≥ 97 %	Merck
Mesitaldehyde	C ₁₀ H ₁₂ O	≥ 90 %	Fluka
5-Bromo-2-thiophenecarboxaldehyde	C ₅ H ₃ BrOS	95 %	Sigma Aldrich
5'-Bromo-2,2'-bithiophene-5-carboxaldehyde	C ₉ H ₃ BrOS ₂	97 %	Sigma Aldrich
4-(Trifluoromethyl)benzaldehyde	C ₈ H ₅ F ₃ O	98 %	Merck
4-(Trifluoromethoxy)benzaldehyde	C ₈ H ₅ F ₃ O	96 %	Sigma Aldrich
4-(Dimethylamino)benzaldehyde	C ₉ H ₁₁ NO	99 %	Merck
4-(1-Piperidiny)benzaldehyde	C ₁₂ H ₁₅ NO	97 %	Sigma Aldrich
2,3-Dihydrobenzofuran-5-carboxaldehyde	C ₉ H ₈ O ₂	97 %	Sigma Aldrich
Acetone	C ₃ H ₆ O	99.5 %	Qrec
Ethanol	C ₂ H ₅ OH	99.5 %	Qrec
Methanol	CH ₃ OH	99.5 %	Qrec
Ethyl acetate	C ₄ H ₈ O ₂	≥ 99 %	Qrec
L-Ascorbic acid	C ₆ H ₈ O ₆	99 %	Sigma Aldrich
2,2-Diphenyl-1-picrylhydrazyl	C ₁₈ H ₁₂ N ₅ O ₆	95 %	Sigma Aldrich
Ethylenediaminetetraacetic acid	C ₁₀ H ₁₆ N ₂ O ₈	99 %	Sigma Aldrich
Ferrous chloride	FeCl ₂	98 %	Sigma Aldrich
Ferrozine	C ₂₀ H ₁₂ N ₄ Na ₂ O ₆ S ₂	97 %	Sigma Aldrich
3,4,5-Trihydroxybenzoic acid	C ₁₀ H ₁₂ O ₅	98 %	Sigma Aldrich
Phosphate buffer saline pellet	C ₁₂ H ₃ K ₂ Na ₃ O ₈ P ₂	≥ 99.9 %	Sigma Aldrich
Hydrogen peroxide	H ₂ O ₂	30 %	Merck
Sodium hydroxide pellet	NaOH	97 %	Merck
Deuterated chloroform	CDCl ₃	≥ 99.9 %	Sigma Aldrich

3.2.2 General Procedure for the Synthesis of 5-Chlorothiophen-2-yl Chalcone (Compounds 1a-1l)

The synthesis process for heterocyclic chalcone analogous (**1a** – **1l**) is shown in Figure 3.2. All compounds were obtained expectedly from a mixture of 2-acetyl-5-chlorothiophene (0.01 mol) and substituted benzaldehyde (0.01 mol) in 8 ml methanol. While the mixture is completely dissolved, catalytic amount of sodium hydroxide was added drop by drop to the mixture solution with vigorous stirring in a 50 ml round-bottom flask. The reaction mixture was stirred for about 6 hours at room temperature. After the stirred process was completed, the mixture was poured into cold water and stirred for 10 minutes. Next, the resultant precipitate products were filtered, washed a few times with distilled water and allow to dry. Single crystals were obtained using the suitable solvent in the crystallization and recrystallization process. Melting points for samples **1a** – **1l** were recorded by using Stuart SMP10 digital melting point apparatus.



Where R is, for

1a = 2-Pyridine

1b = 2-Thiophene

1c = 5-Methyl-2-thiophene

1d = 4-(Methylthio)benzene

1e = Mesitylene

1f = 5-Bromo-2-thiophene

1g = 5'-Bromo-2,2'bithiophene

1h = 4-(Trifluoromethyl)benzene

1i = 4-(Trifluoromethoxy)benzene

1j = 4-(Dimethylamino)benzene

1k = 4-(1-Piperidinyl)benzene

1l = 2,3-Dihydrobenzofuran

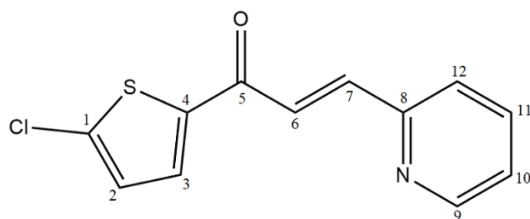
Figure 3.2 Schematic diagram for synthesis of heterocyclic chalcone derivatives.

3.3 Spectroscopic Studies

Spectroscopy is a technique to study the interactions occur between the matter and the electromagnetic radiation. It enables researcher to characterize the studied compounds through combination of different spectroscopy tools. Therefore, the invention of spectroscopy tools has enhanced the development of organic chemistry and they are widely used in the determination of the structure of organic compounds. Two types of spectroscopy tools are used in this research project to characterize the molecular structure which include Fourier transform infrared (FT-IR) spectroscopy and the nuclear magnetic resonance (NMR) spectroscopy (proton and carbon-13).

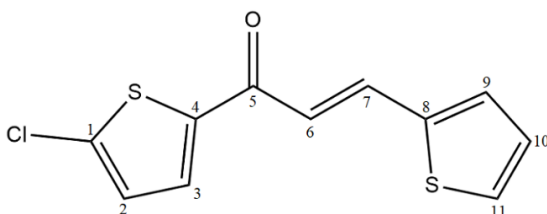
All compounds were subjected to Fourier transform infrared (FT-IR) and nuclear magnetic resonance (NMR) spectroscopy to ensure the chemical structure of these synthesized products are as postulated. The Fourier transform infrared spectroscopy (FT-IR) spectra were analysed by Perkin Elmer Frontier FTIR Spectrometer equipped with attenuated total reflection (ATR) in frequency range of 600 - 4000 cm^{-1} . Whereas, ^1H and ^{13}C nuclear magnetic resonance (NMR) spectra were determined by Bruker Avance III 500 spectrometer with deuterated chloroform (CDCl_3) as solvent in frequencies of 500 MHz and 125 MHz, respectively. Spectrum (*Spectrum*, 2011) was used to analyse the raw data of FT-IR, while Delta (*Delta 5.0.4*, 2014) was applied to classify the atoms in NMR spectra. The spectra results were obtained as following:

(E)-1-(5-chlorothiophen-2-yl)-3-(pyridin-2-yl)prop-2-en-1-one (**1a**):



Solvent used to form single crystal: Acetone; Yield: 66%; M.P.: 127 °C -129 °C; FT-IR (ATR(solid)cm⁻¹): 3047 ν (Ar C-H), 1651.5 ν (C=O), 1596.4, 1420.5 ν (Ar C=C), 1227.6 ν (C-N), 774 ν (C-Cl), 679 ν (C-S); ¹H-NMR (500 MHz, CDCl₃): δ 8.683-8.671 (d, 1H, J= 4.6 Hz, ³CH), 7.935-7.897 (d, 1H, J= 15.6 Hz ⁷CH), 7.793-7.723 (m, 3H, ⁶CH, ⁹CH and ¹¹CH overlapped), 7.466-7.447 (d, 1H, J=7.2 Hz, ¹²CH), 7.323-7.289 (t, 1H, J=7.2 Hz, ¹⁰CH), 7.013-7.002 (d, 1H, J= 4.6 Hz, ²CH); ¹³C-NMR (125 MHz, CDCl₃): 181.39 (C5), 152.87 (C8), 150.28 (C9), 144.31 (C4), 142.44 (C7), 140.43 (C1), 137.06 (C3), 132.09 (C11), 127.90 (C2), 125.90 (C6), 124.72 (C12), 124.15 (C10)

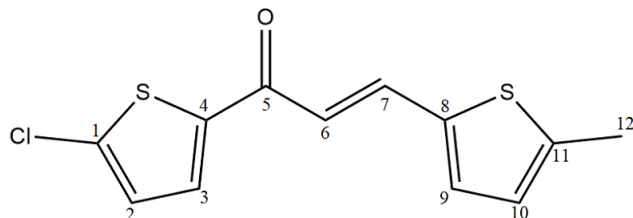
(E)-1-(5-chlorothiophen-2-yl)-3-(thiophen-2-yl)prop-2-en-1-one (**1b**)



Solvent used to form single crystal: Acetone; Yield: 70%; M.P.: 92 °C -94 °C; FT-IR (ATR(solid)cm⁻¹): 3081 ν (Ar C-H), 1639.2 ν (C=O), 1571.6, 1413.6 ν (Ar C=C), 799.9 ν (C-Cl), 694.1 ν (C-S); ¹H-NMR (500 MHz, CDCl₃): δ 7.965-7.924 (d, 1H, , J=16.4 Hz, ⁷CH), 7.617-7.608 (d, 1H, J= 3.4 Hz, ¹¹CH), 7.438-7.425 (d, 1H, J= 4.6 Hz ³CH), 7.367-7.359 (d, 1H, J= 3.4 Hz, ⁹CH), 7.117-7.079 (m, 2H, ⁶CH and ¹⁰CH overlapped), 7.000-6.990 (d, 1H, J= 4.6 Hz, ²CH); ¹³C-NMR (125 MHz, CDCl₃): 180.68 (C5),

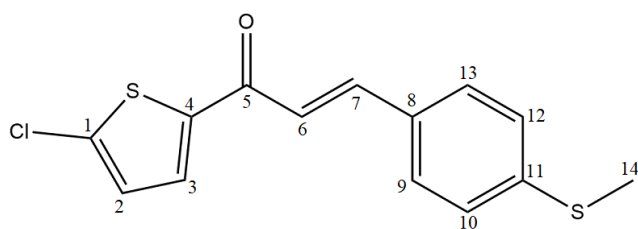
144.30 (C4), 140.05 (C1), 139.77 (C8), 136.95 (C3), 132.59 (C9), 131.14 (C7), 129.26 (C2), 128.55 (C11), 127.78 (C6), 119.17 (C10).

(E)-1-(5-chlorothiophen-2-yl)-3-(5-methylthiophen-2-yl)prop-2-en-1-one (**1c**)



Solvent used to form single crystal: Acetone; Yield: 64%; M.P.: 108 °C -110 °C; FT-IR (ATR(solid)cm⁻¹): 3078 ν (Ar C-H), 2916.8, 2857.9 ν (CH₃), 1652.2 ν (C=O), 1574.8, 1419.8 ν (Ar C=C), 793.7 ν (C-Cl), 706.9 ν (C-S); ¹H-NMR (500 MHz, CDCl₃): δ 7.882-7.844 (d, 1H, J= 15.2 Hz, ⁷CH), 7.584-7.574 (d, 1H, J= 4.4 Hz, ³CH), 7.171-7.162 (d, 1H, J= 3.6 Hz, ⁹CH), 6.986-6.938 (m, 2H, ⁶CH and ¹⁰CH overlapped), 6.755-6.743 (d, 1H, J=4.4 Hz, ²CH), 2.523 (s, 3H, ¹²CH₃); ¹³C-NMR (125 MHz, CDCl₃): 180.73 (C5), 145.17 (C4), 144.49 (C11), 139.43 (C1), 138.11 (C8), 137.41 (C3), 133.54 (C9), 130.88 (C7), 127.73 (C2), 127.09 (C6), 117.82 (C10), 16.04 (C12)

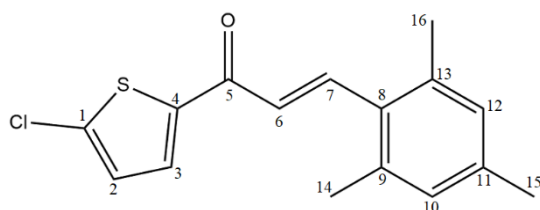
(E)-1-(5-chlorothiophen-2-yl)-3-(4-(methylthio)phenyl)prop-2-en-1-one (**1d**)



Solvent used to form single crystal: Acetone; Yield: 68%; M.P.: 129 °C -131 °C; FT-IR (ATR(solid)cm⁻¹): 3078 ν (Ar C-H), 2985, 2832 ν (CH₃), 1645 ν (C=O), 1575, 1420 ν (Ar C=C), 794 ν (C-Cl), 729 ν (C-S); ¹H-NMR (500 MHz, CDCl₃): δ 7.794-7.756 (d, 1H, J= 15.2 Hz, ⁷CH), 7.622-7.612 (d, 1H, J= 4.0 Hz, ³CH), 7.536-7.515 (d, 2H, J= 8.4 Hz ⁹CH and ¹³CH overlapped), 7.275-7.228 (m, 3H, ⁶CH, ¹⁰CH and ¹²CH

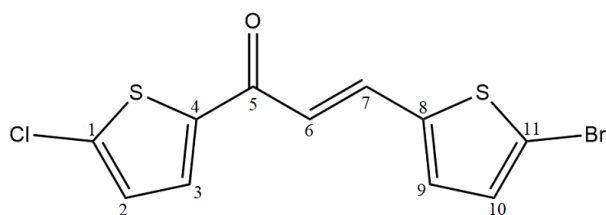
overlapped), 6.995-6.985 (d, 1H, $J=4.0$ Hz, ^2CH), 2.506 (s, 3H, $^{14}\text{CH}_3$); ^{13}C -NMR (125 MHz, CDCl_3): 181.07 (C5), 144.44 (C4), 144.07 (C7), 142.91 (C1), 139.69 (C11), 131.11 (C3), 131.02 (C8), 128.98 (C9 and C13 overlapped), 127.77 (C2), 126.00 (C10 and C12 overlapped), 119.27 (C6), 15.17 (C14)

(E)-1-(5-chlorothiophen-2-yl)-3-mesitylprop-2-en-1-one (**1e**)



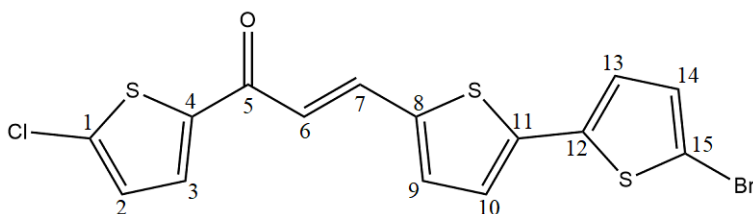
Solvent used to form single crystal: Acetone; Yield: 74%; M.P.: 107 °C -109 °C; FT-IR (ATR(solid) cm^{-1}): 3078 $\nu(\text{Ar C-H})$, 2916.7, 2864 $\nu(\text{CH}_3)$, 1643.8 $\nu(\text{C=O})$, 1591.4, 1417.6 $\nu(\text{Ar C=C})$, 799.9 $\nu(\text{C-Cl})$, 719.3 $\nu(\text{C-S})$; ^1H -NMR (500 MHz, CDCl_3): δ 8.014-7.975 (d, 1H, $J= 15.6\text{Hz}$, ^7CH), 7.551-7.541 (d, 1H, $J= 4.0$ Hz, ^3CH), 6.992-6.921 (m, 4H, ^2CH , ^6CH , ^{10}CH and ^{12}CH overlapped), 2.379 (s, 6H, $^{14}\text{CH}_3$ and $^{16}\text{CH}_3$ overlapped), 2.299 (s, 3H, $^{15}\text{CH}_3$); ^{13}C -NMR (125 MHz, CDCl_3): 181.23 (C5), 144.36 (C4), 143.12 (C7), 139.78 (C1), 138.97 (C11), 137.39 (C3), 131.27 (C10 and C12 overlapped), 129.47 (C8, C9 and C13 overlapped), 127.81 (C2), 125.66 (C6), 21.34 (C14 and C16 overlapped), 21.206 (C15).

(E)-3-(5-bromothiophen-2-yl)-1-(5-chlorothiophen-2-yl)prop-2-en-1-one (**1f**)



Solvent used to form single crystal: Ethyl Acetate; Yield: 70%; M.P.: 135 °C -137 °C; FT-IR (ATR(solid) cm^{-1}): 3084.1 ν (Ar C-H), 1646 ν (C=O), 1584, 1416.7 ν (Ar C=C), 790.6 ν (C-Cl), 703.8 ν (C-S), 610.8 ν (C-Br); $^1\text{H-NMR}$ (500 MHz, CDCl_3): δ 7.820 – 7.782 (d, 1H, $J=15.2$ Hz, ^7CH), 7.589 – 7.578 (d, 1H, $J=4.4$ Hz, ^3CH), 7.101 – 7.091 (d, 1H, $J=4.0$ Hz ^9CH), 7.054 – 7.044 (d, 1H, $J=4.0$ Hz, ^{10}CH), 6.998 – 6.959 (m, 2H, ^2CH and ^6CH overlapped); $^{13}\text{C-NMR}$ (125 MHz, CDCl_3): 180.38 (C5), 144.10 (C4), 141.590 (C1), 140.06 (C8), 135.98 (C9), 132.84 (C3), 131.53 (C7), 131.254 (C10), 127.84(C2), 119.41 (C6), 116.91 (C11).

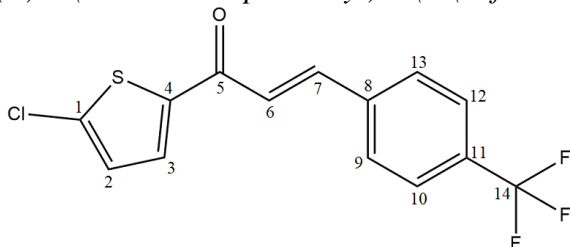
(E)-3-(5'-bromo-[2,2'-bithiophen]-5-yl)-1-(5-chlorothiophen-2-yl)prop-2-en-1-one (**1g**)



Solvent used to form single crystal: Acetone; Yield: 78%; M.P.: 189 °C -190 °C; FT-IR (ATR(solid) cm^{-1}): 3074.8 ν (Ar C-H), 1635 ν (C=O), 1577.8, 1419.8 ν (Ar C=C), 781.3 ν (C-Cl), 703.8 ν (C-S); $^1\text{H-NMR}$ (500 MHz, CDCl_3): δ 7.889 – 7.851 (d, 1H, $J=15.2$ Hz, ^7CH), 7.612 – 7.601 (d, 1H, $J=4.4$ Hz, ^3CH), 7.103 – 7.056 (m, 2H, ^9CH and ^{10}CH overlapped), 7.034 – 6.994 (m, 4H, ^2CH , ^6CH , ^{13}CH and ^{14}CH overlapped); $^{13}\text{C-NMR}$ (125 MHz, CDCl_3): 180.43 (C5), 144.31 (C4), 139.91 (C1), 138.99 (C12),

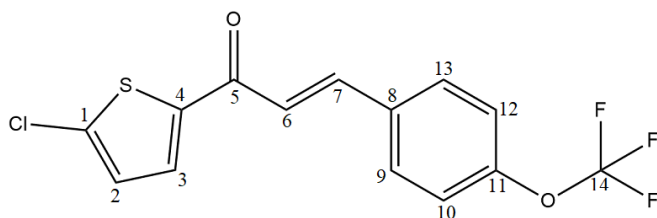
138.12 (C11), 136.52 (C8), 133.87 (C3), 131.10 (C7), 127.81 (C10), 126.31 (C14),
125.11 (C9), 124.92 (C2), 124.48 (C13), 119.04 (C6), 112.91 (C15)

(E)-1-(5-chlorothiophen-2-yl)-3-(4-(trifluoromethyl)phenyl)prop-2-en-1-one (**1h**)



Solvent used to form single crystal: Acetone; Yield: 72%; M.P.: 124 °C -126 °C; FT-IR (ATR(solid)cm⁻¹): 3081 ν (Ar C-H), 1647.6 ν (C=O), 1593.3, 1416.8 ν (Ar C=C), 1111.6 ν (C-F), 799.9 ν (C-Cl), 740.6 (C-S); ¹H-NMR (500 MHz, CDCl₃): δ 7.832 – 7.793 (d, 1H, J= 15.6 Hz, ⁷CH), 7.723 – 7.702 (d, 2H, J= 8.4 Hz, ⁹CH and ¹³CH overlapped), 7.670 – 7.648 (m, 3H, ³CH, ¹⁰CH and ¹²CH overlapped), 7.385 – 7.346 (d, 1H, J= 15.6 Hz, ⁶CH), 7.017 – 7.007 (d, 1H, J= 4.0 Hz, ²CH); ¹³C-NMR (125 MHz, CDCl₃): 180.69 (C5), 143.91 (C4), 142.54 (C7), 140.54 (C1), 137.96 (C8), 132.34 (C14), 132.09 (C14), 131.71 (C3), 128.67 (C6, C10 and C12 overlapped), 127.93 (C9 and C13 overlapped), 126.01 (C11), 125.22 (C14), 122.65 (C2), 122.51 (C14).

(E)-1-(5-chlorothiophen-2-yl)-3-(4-(trifluoromethoxy)phenyl)prop-2-en-1-one (**1i**)



Solvent used to form single crystal: Acetone; Yield: 66%; M.P.: 119 °C -121 °C; FT-IR (ATR(solid)cm⁻¹): 3082.3 ν (Ar C-H), 1652.2 ν (C=O), 1579.3, 1419.8 ν (Ar C=C), 1156.3 ν (C-F), 1016.5 ν (C-O), 799.9 ν (C-Cl), 750.3 ν (C-S); ¹H-NMR (500 MHz, CDCl₃): δ 7.798 – 7.759 (d, 1H, J= 15.6 Hz, ⁷CH), 7.650 – 7.626 (m, 3H, ³CH, ⁹CH